

On the Effect of Low-Rank Weights on Adversarial Robustness of Neural Networks

Peter Langenberg, Emilio Rafael Balda, Arash Behboodi, and Rudolf Mathar*

October 7, 2021

Abstract

Recently, there has been an abundance of works on designing Deep Neural Networks (DNNs) that are robust to adversarial examples. In particular, a central question is which features of DNNs influence adversarial robustness and, therefore, can be used to design robust DNNs. In this work, this problem is studied through the lens of compression which is captured by the low-rank structure of weight matrices. It is first shown that adversarial training tends to promote simultaneously low-rank and sparse structure in the weight matrices of neural networks. This is measured through the notions of effective rank and effective sparsity. In the reverse direction, when the low rank structure is promoted by nuclear norm regularization and combined with sparsity inducing regularizations, neural networks show significantly improved adversarial robustness. The effect of nuclear norm regularization on adversarial robustness is paramount when it is applied to convolutional neural networks. Although still not competing with adversarial training, this result contributes to understanding the key properties of robust classifiers.

1 Introduction

In recent years, deep neural networks (DNNs) have greatly improved the state-of-the-art performance of a variety of tasks in computer vision (He et al., 2015) and automatic speech recognition (Xiong et al., 2017), medical imaging (Litjens et al., 2017) (Esteva et al., 2017), robotics (Sünderhauf et al., 2018) (Giusti et al., 2016) and game playing (Silver et al., 2017). However, it has been shown that very small additive perturbations of the input sample, known as *adversarial* perturbations, can cause DNN based vision systems to fail (Szegedy et al., 2014) (Goodfellow et al., 2015). Such intentionally perturbed versions of clean samples that fool DNNs are referred to as *adversarial examples*. The robustness of DNNs against these attacks has recently received significant attention.

Different hypotheses have been made about the existence of adversarial examples. In (Goodfellow et al., 2015), it is hypothesized that DNNs are particularly vulnerable to adversarial examples because of their too linear decision boundary in the vicinity around the data points together with the assumption of sufficiently large dimensionality of the problem. In (Tanay & Griffin, 2016), however, it is shown that it is possible to train linear classifiers that are resistant to adversarial attacks which stands in contrast to the linearity hypothesis. Moreover, it is exemplified that high dimensional problems are not necessarily more sensitive to adversarial examples. Further, (Sabour et al., 2016) manipulated deep representations instead of the input and argued that the linearity hypothesis is not sufficient to explain this type of attack. Regarding the observed transferability of adversarial examples across different DNN architectures (Szegedy et al., 2014) and (Tramèr et al., 2017) propose a method for estimating the dimensionality of the space of adversarial examples. It is shown that adversarial examples span a contiguous subspace

*Institute for Theoretical Information Technology (TI), RWTH Aachen University.

of large dimensionality. Further, it is shown that those subspaces intersect for different DNNs that have common adversarial examples. (Fawzi et al., 2015) propose the low flexibility of DNNs, compared to the difficulty of the classification task, as a reason for the existence of adversarial examples. (Fawzi et al., 2016) suggest that the flatness of the decision boundary is a reason for the existence of adversarial examples. Another perspective is proposed in (Tanay & Griffin, 2016) with the *boundary tilting* mechanism. It is argued that adversarial examples exist when the decision boundary lies close to the sub-manifold of sampled data. The notion of *adversarial strength* is introduced which refers to the deviation angle between the target classifier and the nearest centroid classifier. It is shown that the adversarial strength can be arbitrarily increased independently of the classifier’s accuracy by tilting the boundary. (Rozsa, Günther, & Boulton, 2016) give another explanation arguing that over the course of training the correctly classified samples do not have a significant impact on shaping the decision boundary and eventually remain close to it. This phenomenon is called evolutionary stalling. In (Rozsa, Günther, & Boulton, 2016), the correlation between robustness and accuracy of the classifier is studied empirically by attacking different state-of-the-art DNNs. It is observed that higher accuracy DNNs are more sensitive to adversarial attacks than lower accuracy ones. Regarding universal adversarial examples, (Moosavi-Dezfooli et al., 2017) show empirically and (Moosavi-Dezfooli et al., 2018) formally that their existence is partly caused by the correlation between the normals to the decision boundary in the vicinity of natural images, i.e. these normals span a low dimensional space. It is found that in this subspace the decision boundary is positively curved in the vicinity of natural images. In that work, (Moosavi-Dezfooli et al., 2018) assume that the first order linear approximation of the decision boundary holds locally in the vicinity of natural images. However, (Moosavi-Dezfooli et al., 2018) show also that this model is not sufficient to explain large fooling ratios. The authors introduce the locally curved decision boundary model which indicates that DNNs are particularly vulnerable to universal perturbations in shared directions along which the decision boundary is systematically positively curved, i.e. there exists a subspace where the decision boundary is positively curved in the vicinity of natural images along most directions in this subspace.

In (Kurakin et al., 2017) and (Madry et al., 2018), evidence was given that increasing model capacity alone can help to induce DNNs to be more robust against adversarial attacks. Further, it was observed that robust models (obtained by adversarial training) exhibit rather sparse weights compared to unrobust ones. (Madry et al., 2018) compare the weights of a CNN that is trained naturally vs. adversarially on the MNIST dataset (LeCun & Cortes, 2010). After training, it is observed that the adversarially trained CNN has more sparse weights in the first two convolutional filters than the naturally trained one. (Gopalakrishnan et al., 2018; Marzi et al., 2018) propose that producing sparse input representations improves the robustness of linear and deeper binary classifiers. (Guo et al., 2018) conduct a more detailed study of the relation between sparsity and robustness of DNNs. It is shown formally and empirically that more sparse DNNs are more robust against adversarial attacks, up to a certain limit where robustness starts decreasing again. Recently, (Sanyal et al., 2018) have provided evidence that adversarial robustness can be improved by encouraging the learned representations to lie in a low-rank subspace. We see that there are many different hypotheses about the nature of adversarial examples which, in fact, do not perfectly match. This makes the research on the nature of adversarial examples an active area. Inspired by recent works (Madry et al., 2018; Guo et al., 2018; Sanyal et al., 2018) in this work we suggest that one should design robust DNNs considering the *effective sparsity* and the *effective rank* of the weights. We observe that adversarial training leads to low-rank and sparse weights. So far, these two properties have not been pointed out together in the context of adversarial robustness of DNNs. We are able to substantially improve adversarial robustness by simultaneously promoting low-rank and sparse weights using different regularization techniques. Moreover, we raise an open question whether there is an optimal combination of sparsity and low-rankness of the weights that can further improve robustness. We believe that simultaneous

sparsity and low-rankness of the weights play a significant role in robustness, but do not fully explain the success of adversarial training.

2 Preliminaries

Let $\mathbf{x} \in \mathcal{X} \subseteq \mathbb{R}^n$ to be a random n -dimensional vector representing the input of classifiers, which belongs to some set of possible inputs \mathcal{X} . Furthermore, we denote $\hat{\mathbf{y}} \in \mathcal{Y}$ to be the output label assigned by a classifier, which belongs to some discrete set \mathcal{Y} of possible labels. Then a classifier consists of some function $f : \Theta \times \mathcal{X} \rightarrow \mathcal{Y}$ such that $\hat{\mathbf{y}} = f(\theta; \mathbf{x})$ where $\theta \in \Theta$ contains all tunable model parameters in the hypothesis space Θ . In the case of DNN of m layers the set of tunable parameters is given by $\theta = \{W^1, \dots, W^m\}$ where W^i are matrices with appropriate dimensions such that the neural network function f has the form

$$f(\theta; \mathbf{x}) = \varphi(W^m \varphi(W^{m-1}(\dots \varphi(W^1 \mathbf{x}))) \dots),$$

where $\varphi : \mathbb{R} \rightarrow \mathbb{R}$ is an activation function that is applied to vectors in a point-wise manner. For the sake of notation let $i \in [m]$ be the layer index, m the number of hidden and output layers, and m^i the number of neurons of layer i . The vectors $\mathbf{t}^i \in \mathbb{R}^{m^i} \forall i \in \{1, \dots, m-1\}$ are called hidden representations, given by

$$\mathbf{t}^i = \varphi(W^i \mathbf{t}^{i-1}), \quad \forall i = 1, \dots, m, \quad (1)$$

with $\mathbf{t}^0 = \mathbf{x}$ and $\hat{\mathbf{y}} = \mathbf{t}^m$. Each layer is represented by its own weight matrix $W^i \in \mathbb{R}^{m^i \times m^{i-1}}$ that defines the mapping from \mathbf{t}^{i-1} to \mathbf{t}^i . In this work, we refer to Fully Connected Neural Networks (FCNNs) to the DNNs that only contain fully-connected layers, while Convolutional Neural Networks (CNNs) are DNNs containing convolutional filters. We use the operators $\|\cdot\|_F$, $\|\cdot\|_*$ and $\|\cdot\|_1$ to denote the Frobenius, nuclear and ℓ_1 norms respectively. The effective sparsity of a matrix W is given by

$$\bar{s}(W) = \frac{\|W\|_1}{\|W\|_F}. \quad (2)$$

The definition applies to vectors as well with $\bar{s}(\mathbf{x}) = \frac{\|\mathbf{x}\|_1}{\|\mathbf{x}\|_2}$. Note that if a vector \mathbf{x} is s -sparse, i.e., has only s non-zero values, we have $\|\mathbf{x}\|_1 \leq \sqrt{s}\|\mathbf{x}\|_2$. In that sense, this notion is commonly used in compressed sensing as an extension of standard sparsity, see (Gopi et al., 2013). Similarly, the effective sparsity of the vector of singular values of a matrix W is called the effective rank of such matrix, that is

$$\bar{r}(W) = \frac{\|W\|_*}{\|W\|_F}. \quad (3)$$

which is a continuous relaxation of the notion of rank.

Studying DNNs by measuring information theoretic quantities during their training phase has been initiated by (Tishby & Zaslavsky, 2015; Shwartz-Ziv & Tishby, 2017). The authors propose that the hidden representations \mathbf{t}^i of a DNN form the following Markov Chain

$$(\mathbf{x}, \mathbf{y}) \rightarrow \mathbf{t}^1 \rightarrow \dots \rightarrow \mathbf{t}^{m-1} \rightarrow \hat{\mathbf{y}}. \quad (4)$$

Such successive representations are studied with the notion of *mutual information*, which quantifies how much information about one random variable can be obtained if the other random variable is observed. We use the notation $I(\mathbf{a}; \mathbf{b})$ for the mutual information between two random variables \mathbf{a}, \mathbf{b} . Using this quantity, the authors study the behavior of the so called *information plane* which is the 2-dimensional plane of values between successive representations and the input $I(\mathbf{t}^i; \mathbf{x})$ and the output $I(\mathbf{t}^i; \mathbf{y})$ of DNNs during training. In this context, the hidden representation \mathbf{t}^i is seen as a compressed version of \mathbf{x} , where information is lost during compression. Then, $I(\mathbf{t}^i; \mathbf{x})$ quantifies the amount of information about \mathbf{x} that is contained in \mathbf{t}^i . Even though this

paper focuses on the low-rankness and sparsity of the weights to quantify compression, we show experimentally that our findings align with the information theoretic notion of compression, which is measured using mutual information.

3 Simultaneous Low-Rankness and Sparsity in Linear Models: An Example

Consider the case of linear binary classifiers as an example. Let $y \in \{-1, +1\}$ be the random variable corresponding to the label of an input $\mathbf{x} \in \mathbb{R}^n$. The linear classifier with parameter $\mathbf{w} \in \mathbb{R}^n$ assigns the label $\hat{y} = \text{sign}(\mathbf{w}^T \mathbf{x})$ to an input \mathbf{x} . Note that we neglect the bias term b as in $\text{sign}(\mathbf{w}^T \mathbf{x} + b)$ since it can be easily included by appending a scalar 1 to the input vector \mathbf{x} . Therefore, the expected error of this classifier, denoted by $p_0(\mathbf{w})$, is given by

$$p_0(\mathbf{w}) = P(\mathbf{w}^T \mathbf{x} \cdot y < 0).$$

An ℓ_∞ adversarial attack against this classifier is obtained by an input perturbations $\boldsymbol{\eta}$ whose ℓ_∞ -norm is bounded by some $\varepsilon > 0$. The adversarial error is characterized by the following probability:

$$p_\varepsilon(\mathbf{w}) = \max_{\boldsymbol{\eta}: \|\boldsymbol{\eta}\|_\infty \leq \varepsilon} P(\mathbf{w}^T (\mathbf{x} + \boldsymbol{\eta}) \cdot y < 0).$$

The probability $p_\varepsilon(\mathbf{w})$ is a measure of robustness for linear classifiers. The goal is to minimize the error by an appropriate choice of \mathbf{w} . A typical choice of $\boldsymbol{\eta}$ is given by the so called Fast Gradient Sign Method (FGSM) attack for which $\boldsymbol{\eta} = -y\varepsilon \text{sign}(\mathbf{w})$. It was previously discussed in (Guo et al., 2018) that the robustness of linear classifiers are upper bounded by the inverse of $\|\mathbf{w}\|_1$. Since the ℓ_1 -norm is widely used as a sparsity promoting regularization, the authors concluded that the sparsity of \mathbf{w} contributes to the robustness of classifiers against ℓ_∞ attacks. As a matter of fact it can be seen that the robustness to attacks with a bounded norm is related to small dual norm of \mathbf{w} . In this work, we show that the robustness can be improved if the sparsity is complemented with an adequate dimensionality reduction. Although the example of binary linear classifiers is only considered, the result can be also extended to the multi-class setup similar to (Guo et al., 2018).

In most cases, high dimensional data belong to a low dimensional manifold. In this section, we assume that the data lie in a d -dimensional subspace $\mathcal{V} \subset \mathbb{R}^n$ spanned by d orthonormal basis $\mathbf{v}_1, \dots, \mathbf{v}_k$ with $k < n$. However, since the distribution of data is unknown, the dimensionality of data is not known. Therefore, we apply an intermediate linear transformation Q on the data and try to reduce the dimensionality based on the training samples. The classifier is then applied to $Q\mathbf{x}$ for $\mathbf{x} \in \mathbb{R}^n$. The main question is whether this compression step affects adversarial robustness. Intuitively an ℓ_∞ -norm attack allows for ε perturbation of each entry which can translate each data point at by the distance of $\varepsilon\sqrt{n}$ in the space. For higher dimension n , ℓ_∞ -norm attacks can create a bigger overall perturbation of the points. Therefore reducing the effective dimension seems to be favorable to adversarial robustness. A first choice of $Q \in \mathbb{R}^{n \times n}$ can be the orthogonal projection matrix onto the data subspace \mathcal{V} defined by

$$Q = \sum_{i=1}^k \mathbf{v}_i \mathbf{v}_i^T.$$

The following theorem shows that under certain assumptions, this projection can indeed improve the robustness even further.

Theorem 1. *For a binary classification task, suppose that the data samples belong to k -dimensional subspace \mathcal{V} and $Q \in \mathbb{R}^{n \times n}$ is the orthogonal projection onto this subspace. Then, for any given binary linear classifiers with the parameter \mathbf{w} , if the effective sparsity of \mathbf{w} after projection satisfies $\bar{s}(Q\mathbf{w}) \leq \bar{s}(\mathbf{w})$, then*

- The accuracy remains unchanged, i.e.,

$$p_0(\mathbf{w}) = p_0(Q\mathbf{w}).$$

- The adversarial robustness against ℓ_∞ -attacks is either improved or unchanged, i.e.,

$$p_\varepsilon(Q\mathbf{w}) \leq p_\varepsilon(\mathbf{w}).$$

Remark 1. Before stating the proof, some remarks are in order. First of all, note that the new classifier applies to the projected vectors $Q\mathbf{x}$. Since Q is symmetric, this amounts to a new binary classifier with parameter $Q\mathbf{w}$. As it will be seen from the proof, if the vector \mathbf{w} already belongs to the data subspace \mathcal{V} , that is, the discriminating hyperplane is orthogonal to \mathcal{V} , then the adversarial robustness remains unchanged. However, this is highly unlikely for most datasets that are noisy and therefore difficult to find exactly this hyperplane among many choices.

Proof. The optimal ℓ_∞ attack for a vector \mathbf{x} with label y is given by $\boldsymbol{\eta} = -\varepsilon \text{sign}(\mathbf{w})$. The adversarial robustness is therefore characterized by

$$\begin{aligned} P(\mathbf{w}^T(\mathbf{x} + \boldsymbol{\eta}) \cdot y > 0) &= P(y \cdot \mathbf{w}^T \mathbf{x} > \varepsilon \|\mathbf{w}\|_1) \\ &= (1 - p_0(\mathbf{w}))P(|\mathbf{w}^T \mathbf{x}| > \varepsilon \|\mathbf{w}\|_1 \mid y \cdot \mathbf{w}^T \mathbf{x} > 0) \end{aligned}$$

First suppose that the same classifier is applied after the orthogonal projection. Note that for all $\mathbf{x} \in \mathcal{V}$, $Q\mathbf{x} = \mathbf{x}$ and since the data belongs to \mathcal{V} , we have $p_0(\mathbf{w}) = p_0(Q\mathbf{w})$. Furthermore, if $\boldsymbol{\eta}$ is chosen according to FGSM, we get:

$$\begin{aligned} P(\mathbf{w}^T Q(\mathbf{x} + \boldsymbol{\eta}) \cdot y > 0) &= P(y \cdot \mathbf{w}^T Q\mathbf{x} > \varepsilon \|Q\mathbf{w}\|_1) \\ &= (1 - p_0(\mathbf{w}))P(|\mathbf{w}^T \mathbf{x}| > \varepsilon \|Q\mathbf{w}\|_1 \mid y \cdot \mathbf{w}^T \mathbf{x} > 0). \end{aligned}$$

If $\|Q\mathbf{w}\|_1 \leq \|\mathbf{w}\|_1$, the theorem follows. Since Q is a projection matrix, for any \mathbf{w} we have that $\|Q\mathbf{w}\|_2 \leq \|\mathbf{w}\|_2$. This inequality and the definition of effective sparsity yield

$$\frac{\|Q\mathbf{w}\|_1}{\bar{s}(Q\mathbf{w})} \leq \frac{\|\mathbf{w}\|_1}{\bar{s}(\mathbf{w})}.$$

Given the initial assumption $\bar{s}(Q\mathbf{w}) \geq \bar{s}(\mathbf{w})$ we get

$$\|Q\mathbf{w}\|_1 \leq \frac{\bar{s}(Q\mathbf{w})}{\bar{s}(\mathbf{w})} \|\mathbf{w}\|_1 \leq \|\mathbf{w}\|_1.$$

Therefore $\varepsilon \|\mathbf{w}\|_1 \geq \varepsilon \|Q\mathbf{w}\|_1$ thus $p_\varepsilon(\mathbf{w}) \geq p_\varepsilon(Q\mathbf{w})$. \square

The condition on effective sparsity is not very demanding. Indeed assume that $\mathcal{V} = \text{span}(\mathbf{e}_1, \dots, \mathbf{e}_k)$ for $k < n$. We have $\|Q\mathbf{w}\|_1 = \sum_{i=1}^k |w_i| \leq \|\mathbf{w}\|_1$. The equality holds only if $\mathbf{w} \in \mathcal{V}$. In other words, if the discriminating hyperplane is not orthogonal to the data subspace, there is always a gain in low dimensional projection. Note that for an arbitrary classifier $f(\cdot)$, the accuracy remains unchanged after the projection. In this case, if the corresponding gradient is projected such that its ℓ_1 norm is reduced after the projection, then the robustness will be increased. Finally, if we overparametrize the classifier $\text{sign}((Q\mathbf{w})^T \mathbf{x})$ as $\text{sign}((QW^1 \dots W^{d-1} \mathbf{w})^T \mathbf{x})$ we obtain a d -layered neural network with linear activations whose initial weight matrix given by QW^1 has low rank. This remark points our attention specially into the low-rankness the first weight matrices.

4 Inducing Compression through Regularization

In Figure 1 and Figure 2, we observe how adversarial training, using the FGSM and Projected Gradient Descent (PGD) attacks, induces effective sparsity as well as effective low-rankness to the weight matrices of a FCNN (details about the simulation setup are provided in section 5). Interestingly, the effective low-rankness of weights coincide with lower mutual information values between the input and hidden representations which can be seen as a form of compression in the information theoretic sense. Motivated by this result, as well as Theorem 1, the question

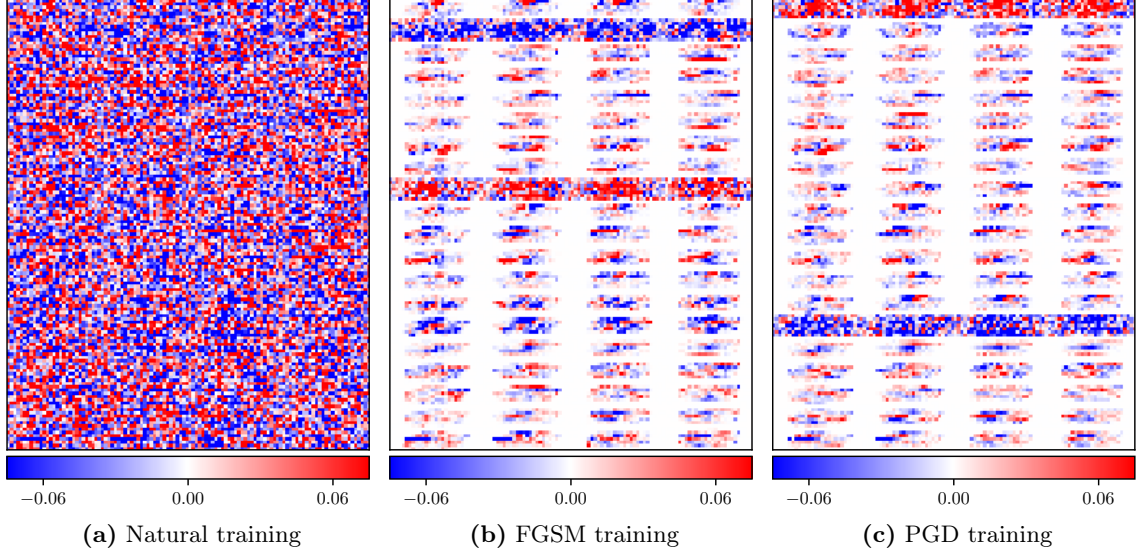


Figure 1: Reshaped input weight matrix $W^1 \in \mathbb{R}^{20 \times 784}$ of the FCNN after natural vs. adversarial training with $\varepsilon = 0.05$.

is whether it is possible to improve the adversarial robustness by promoting sparsity and low-rankness without adversarial training. We introduce three regularization techniques designed to promote sparsity and low-rankness to the weight matrices of DNNs. In order to promote sparsity on the weight matrices, the ℓ_1 -regularization, a common choice for this purpose, is employed:

$$\mathcal{L}_{\ell_1}(\theta, \boldsymbol{\lambda}_1; \mathbf{x}, \mathbf{y}) = \sum_{i=1}^m \lambda_{1,i} \|W^i\|_1, \quad (5)$$

where $\boldsymbol{\lambda}_1 = (\lambda_{1,1}, \dots, \lambda_{1,m}) \in \mathbb{R}_+^m$ is a vector of hyper-parameters. Just like ℓ_1 -regularization is a relaxation of sparsity measure, the nuclear norm is the convex relaxation of rank of a matrix and therefore, the nuclear norm regularization is used to promote low-rankness.

$$\mathcal{L}_{\text{nuclear}}(\theta, \boldsymbol{\lambda}_*; \mathbf{x}, \mathbf{y}) = \sum_{i=1}^m \lambda_{*,i} \|W^i\|_*, \quad (6)$$

with the corresponding hyper-parameters $\boldsymbol{\lambda}_* = (\lambda_{*,1}, \dots, \lambda_{*,m}) \in \mathbb{R}_+^m$.

As discussed in Section 3 and in (Guo et al., 2018) the robustness to ℓ_∞ attacks of multilayer neural networks with linear activations is controlled by the ℓ_1 -norm of the product of its weight matrices, that is $\|W^1 \cdots W^m\|_1$. Motivated by this result, we include into our study the following regularization

$$\mathcal{L}_{\text{joint}}(\theta, \lambda_{\text{joint}}; \mathbf{x}, \mathbf{y}) = \lambda_{\text{joint}} \|W^1 \cdots W^m\|_1 \quad (7)$$

which promotes robustness in linear neural networks. It might lead to robustness for non-linear networks if the linear model is an adequate approximation. Note that $\mathcal{L}_{\text{joint}}(\theta, \lambda_{\text{joint}}; \mathbf{x}, \mathbf{y})$

is cheaper to compute than $\mathcal{L}_{\text{nuclear}}(\theta, \lambda_*; \mathbf{x}, \mathbf{y})$, which makes it a good alternative to avoid computing SVDs during training. Finally, incorporating these regularization losses into one global loss function yields

$$\begin{aligned} \mathcal{L}(\theta; \mathbf{x}, \mathbf{y}) = & \mathcal{L}_{\text{CE}}(\theta; \mathbf{x}, \mathbf{y}) + \mathcal{L}_{\ell_1}(\theta, \lambda_1; \mathbf{x}, \mathbf{y}) \\ & + \mathcal{L}_{\text{nuclear}}(\theta, \lambda_*; \mathbf{x}, \mathbf{y}) + \mathcal{L}_{\text{joint}}(\theta, \lambda_{\text{joint}}; \mathbf{x}, \mathbf{y}). \end{aligned} \quad (8)$$

In Figure 2, we observe how the proposed regularization techniques successfully induce low-

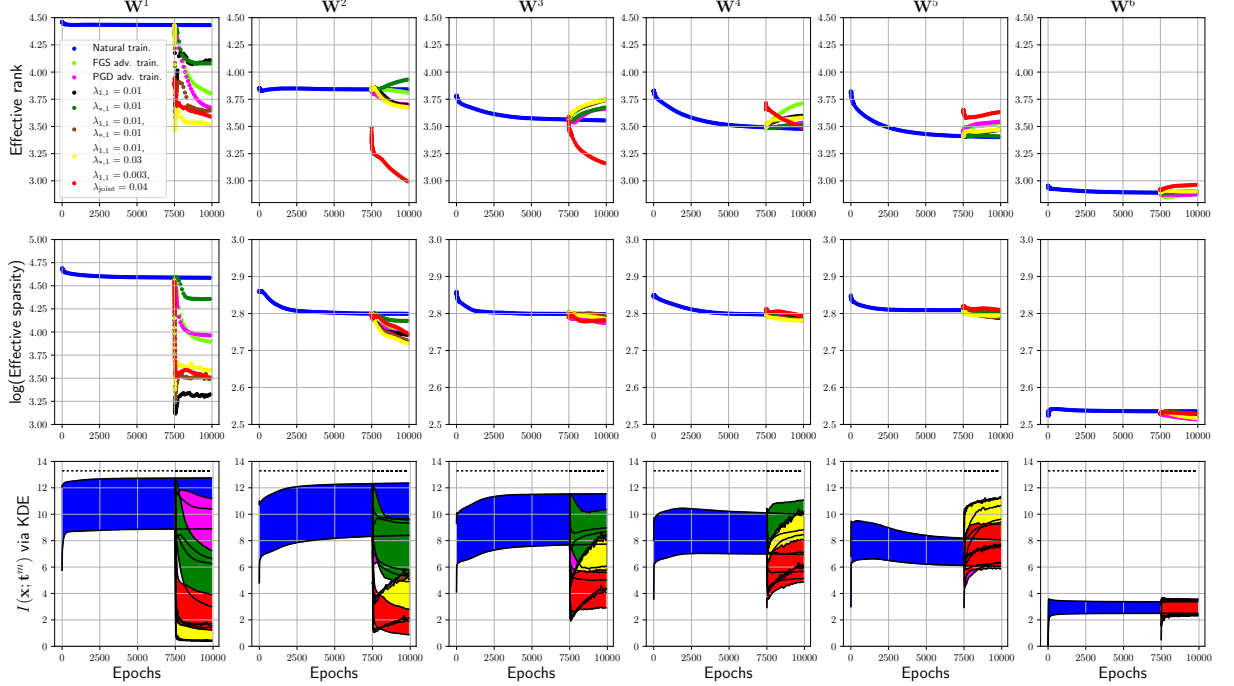


Figure 2: Effective rank, effective sparsity and mutual information of the FCNN.

rankness and sparsity to the weight matrices. At the same time, the mutual information between the input and hidden representations is reduced.

5 Experiments

In this work, we consider two architectures and datasets:

1. **FCNN**: is a fully-connected neural network with 5 hidden layers used on the MNIST handwritten digits dataset (LeCun & Cortes, 2010). Each hidden layer contains 20 neurons with hyperbolic tangent activations, while the output layer uses the softmax function. We use a learning rate of 0.001 and a batch size of 128 for both training from scratch and fine-tuning.
2. **CNN**: is a convolutional neural network applied on the Fashion-MNIST (F-MNIST) clothing articles dataset (Xiao et al., 2017). It is composed two convolution/max-pooling blocks followed by two fully connected layers. Both convolution/max-pooling blocks use 32 convolution filters of window size 3×3 and pooling window of size 2×2 . The first fully connected layer outputs 128 outputs with hyperbolic tangent activations, while the output layer outputs 10 softmax values. We use a batch size of 64 with a learning rate of 0.01 for training from scratch, and 0.001 for fine-tuning.

In both cases stochastic gradient descent is used for minimizing the loss function.

We consider the FGSM (Goodfellow et al., 2015), PGD (Madry et al., 2018) and the gradient-based norm-constrained method (GNM) from (Balda et al., 2018) as adversarial attacks and study their success on DNNs that are trained naturally, adversarially with FGSM/PGD adversarial examples as well as when using the aforementioned regularization techniques (see section 4). The fooling ratio is defined as the percentage of inputs, among the correctly classified ones, whose classification outcome changes after adding adversarial perturbations. This ratio is calculated on the test set as an empirical measure of sensitivity of the classifier against adversarial attacks for a given upper bound ε on the adversarial perturbation. We focus on the low ε regime since small ε corresponds to adversarial examples that are hard to detect by an observer. In such regime the FGSM often leads to similar attacks as PGD since the decision boundary is linear enough in a vicinity around the clean sample. We found that $\varepsilon = 0.05$ was a proper choice that leads to a fooling ratio slightly below 100% in case of natural training for both considered architectures. We generate the attack using the GNM from (Balda et al., 2018) with $T = 5$ iterations, while PGD attacks are generated with $T = 20$ iterations and a step size of $\alpha = 0.005$.

In the spirit of (Madry et al., 2018), we raise the question to what happens to the weights W^i during adversarial training. For both settings, we took the naturally trained models and fine-tuned them adversarially with FGSM and PGD attacks using a fixed $\varepsilon = 0.05$. As expected, adversarial training substantially decreases the fooling ratios. We illustrate the fooling ratios over the whole course of training in Figure 3 and Figure 4 for the FCNN and the CNN respectively. We compute the fooling ratios for different types of attacks using the same fixed $\varepsilon = 0.05$. We also report the test accuracies on clean data (see the Appendix A). For the CNN model we observe slightly lower test accuracies for the adversarially trained models compared to the naturally trained one. In Figure 2 and Figure 5, we present the effective rank and the effective sparsity over the whole course of training for the FCNN and the CNN respectively. In case of the FCNN, we also estimate the mutual information between the input \mathbf{x} and the hidden representations \mathbf{t}^i using the KDE method (Kolchinsky & Tracey, 2017; Kolchinsky et al., 2017) with a noise variance of $\sigma^2 = 0.1$. Note that the KDE method provides upper and lower bounds for mutual information, instead of a single estimate. In case of the FCNN, we find that adversarial training decreases the effective rank and the effective sparsity of some weight matrices as well as the mutual information (see Figure 2). This effect is most visible for the input weight matrix $W^1 \in \mathbb{R}^{20 \times 784}$. This weight matrix is visualized for natural vs. FGSM/PGD adversarial training in Figure 1. While W^1 looks like noise after natural training, it clearly looks like lower-rank and more sparse after FGSM/PGD adversarial training, with strongly correlated pattern visible. We can also observe this effect in an attenuated form for the CNN experiments. Further, FGSM/PGD adversarial training substantially decreases the effective sparsity of the first two convolutional filters $W^1 \in \mathbb{R}^{3 \times 3 \times 1 \times 32}$ and $W^2 \in \mathbb{R}^{3 \times 3 \times 32 \times 32}$ (see Figure 5). Moreover, FGSM/PGD adversarial training slightly decreases the effective rank of W^2 as well. Using PGD adversarial training reduces the effective rank of W^2 more than FGSM adversarial training does as shown in Figure 5. This is also visible in Figure 7 where we visualize W^2 for natural vs. FGSM/PGD adversarial training. The weights after both FGSM and PGD adversarial training look more sparse and slightly lower-rank than after natural training. In addition, the weights after PGD adversarial training look slightly lower-rank than after FGSM adversarial training. From these observations we first conclude that adversarial training leads to compression in the information theoretic sense. Then, we claim the following:

Claim 1. *Adversarial training leads to low-rank and sparse weights.*

Motivated by Claim 1, we mimic adversarial training by promoting low-rank and sparse weights. We are interested on observing the effect of low-rankness and sparsity on the robustness of DNNs. To that end we promote these properties through regularization of the loss function as explained in Section 4. In case of the FCNN, we first only regularize the input weight matrix W^1

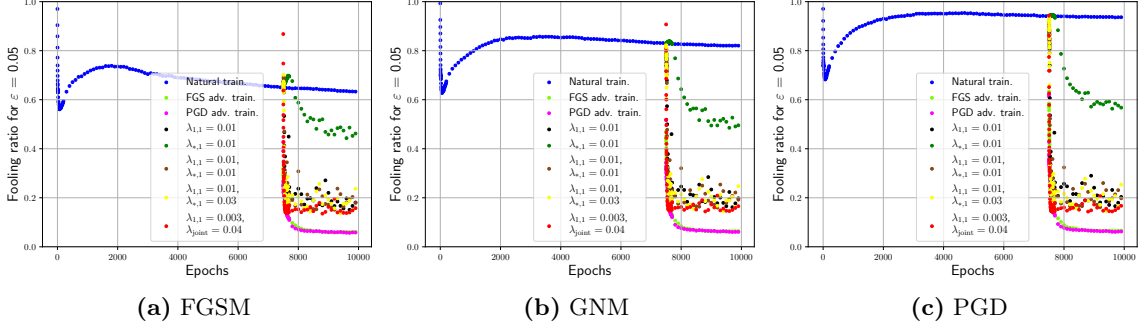


Figure 3: Fooling ratios of the FCNN with respective attack and defense using a fixed $\varepsilon = 0.05$. Dataset: MNIST.

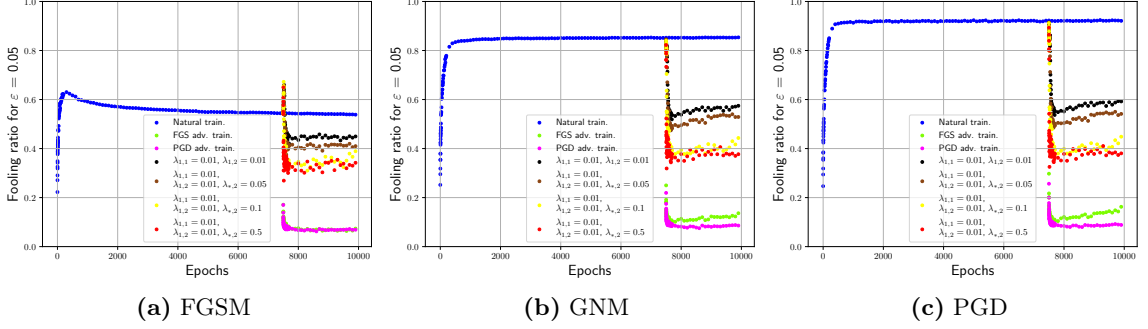


Figure 4: Fooling ratios of the CNN with respective attack and defense using a fixed $\varepsilon = 0.05$. Dataset: F-MNIST.

with different choices of $\lambda_{1,1}$ and $\lambda_{*,1}$ as this weight matrix substantially changes its effective rank and effective sparsity during FGSM/PGD adversarial training. We also provide results on performing only l_1 -regularization on W^1 with $\lambda_{1,1} = 0.01$. Both kinds of regularization substantially decrease the fooling ratios (see Figure 3). As shown in Figure 2, both kinds of regularization substantially decrease the effective sparsity and effective rank of W^1 , as well as W^2 . Surprisingly, performing only l_1 -regularization on W^1 also decreases the effective rank of W^1 . We visualize W^1 after training with both kinds of regularization in Figure 8 indicating sparsity and low-rankness. As shown in Figure 2, we are able to simultaneously decrease the effective rank of W^1 , W^2 and W^3 by using the joint regularization technique (7). Together with explicitly promoting sparsity on W^1 , we are able to again improve robustness compared to regularizing only W^1 . In case of the CNN, we regularize the reshaped versions of the first two convolutional filters W^1 , W^2 (see Appendix B for details about reshaping) with different choices of $\lambda_{1,1}$, $\lambda_{1,2}$ and $\lambda_{*,2}$. We observe a significant improvement in terms of robustness (see Figure 4) when increasing the explicit low-rank promotion on W^2 by nuclear-norm regularization. In Figure 5, we see that a considerably lower effective rank of W^2 can be obtained by adding nuclear-norm regularization. This result further supports that simultaneous sparsity and low-rankness of the weights should be favored on the way towards adversarial robustness. In Figure 9 and Figure 10, we visualize the first and second convolutional filter W^1 , W^2 after training with the different kinds of regularization. These findings support the second claim of this paper.

Claim 2. *Simultaneously low-rank and sparse weights promote robustness against adversarial examples.*

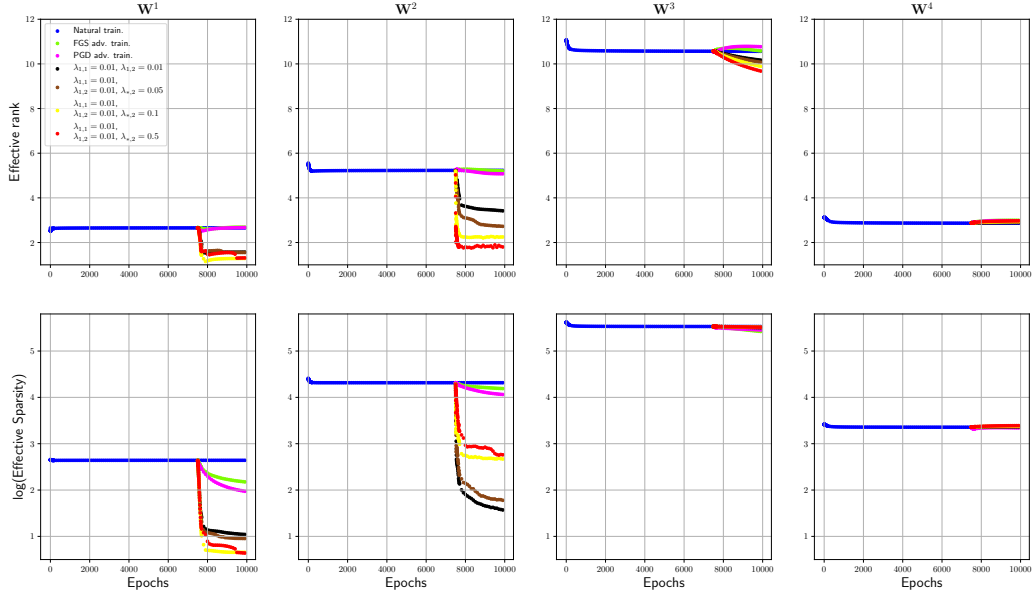


Figure 5: Effective rank and effective sparsity of the CNN.

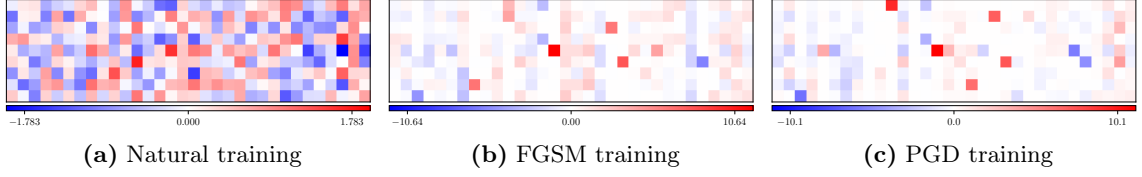


Figure 6: Reshaped input convolutional filter $W^1 \in \mathbb{R}^{3 \times 3 \times 1 \times 32}$ of the CNN after natural vs. adversarial training with $\varepsilon = 0.05$.

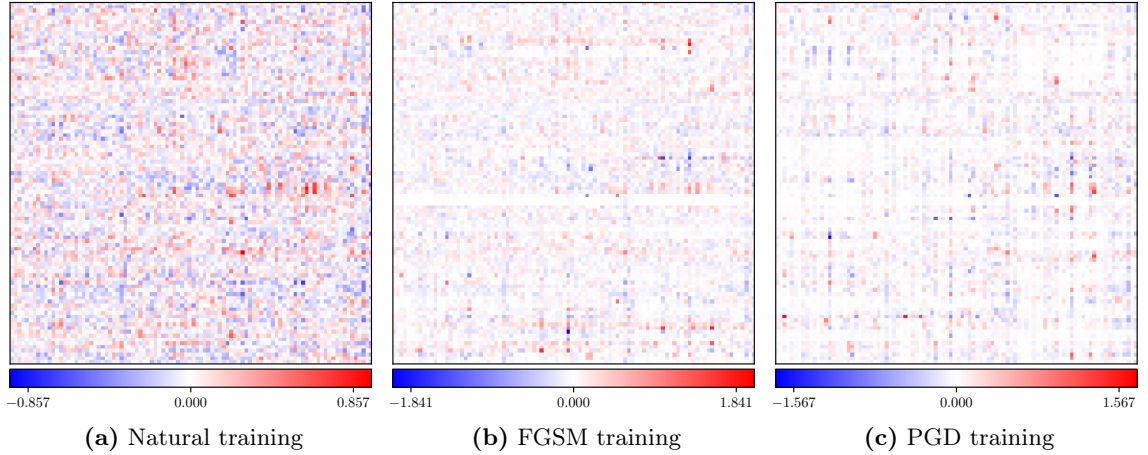


Figure 7: Reshaped second convolutional filter $W^2 \in \mathbb{R}^{3 \times 3 \times 32 \times 32}$ of the CNN after natural vs. adversarial training with $\varepsilon = 0.05$.

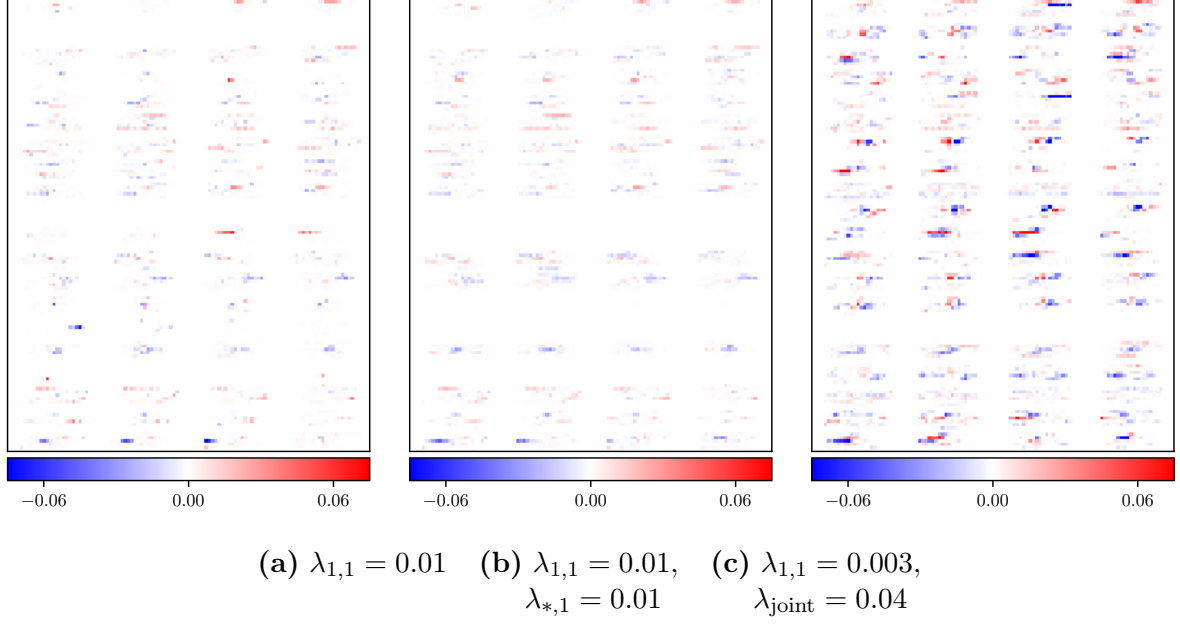


Figure 8: Reshaped input weight matrix $W^1 \in \mathbb{R}^{20 \times 784}$ of the FCNN after training with respective regularization.

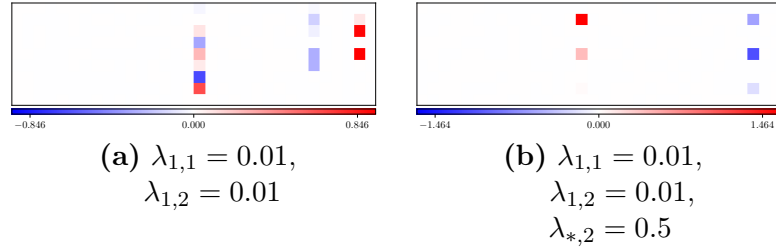


Figure 9: Reshaped input convolutional filter $W^1 \in \mathbb{R}^{3 \times 3 \times 1 \times 32}$ of the CNN after training with respective regularization.

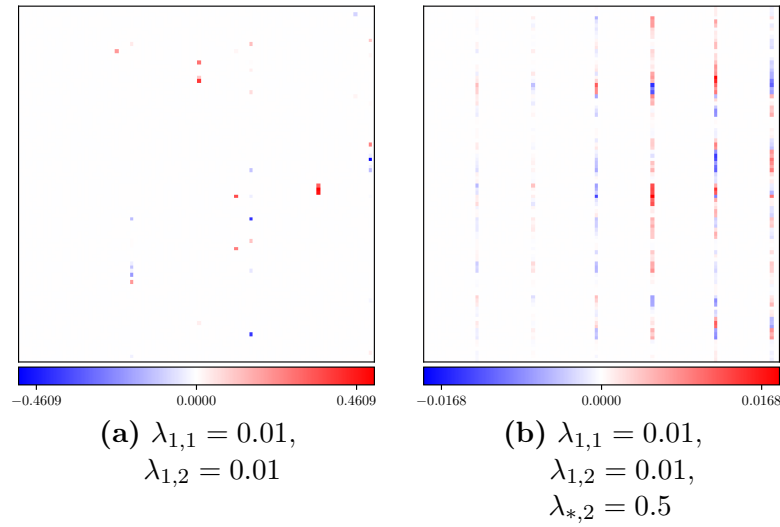


Figure 10: Reshaped second convolutional filter $W^2 \in \mathbb{R}^{3 \times 3 \times 32 \times 32}$ of the CNN after training with respective regularization.

6 Discussion

We are able to obtain more sparse and lower-rank weights by introducing new regularizations. Despite the improvement in adversarial robustness, we cannot still match the robustness of adversarial training. This suggests that beside sparsity and low-rankness of the weights further attributes might be considered. Moreover, it raises an open question whether there is an optimal combination of sparsity and low-rankness of the weights that can further improve robustness. The experiments suggest that, despite their important role, sparsity and low-rankness of the weights do not fully explain the success of adversarial training.

References

- Balda, E. R., Behboodi, A., & Mathar, R. (2018, Oct). On generation of adversarial examples using convex programming. In *52th asilomar conference on signals, systems, and computers*.
- Esteva, A., Kuprel, B., Novoa, R. A., Ko, J., Swetter, S. M., Blau, H. M., & Thrun, S. (2017, January). Dermatologist-level classification of skin cancer with deep neural networks. *Nature*, 542, 115–.
- Fawzi, A., Fawzi, O., & Frossard, P. (2015, 02). Analysis of classifiers’ robustness to adversarial perturbations.
- Fawzi, A., Moosavi-Dezfooli, S.-M., & Frossard, P. (2016). Robustness of classifiers: from adversarial to random noise. In D. D. Lee, M. Sugiyama, U. V. Luxburg, I. Guyon, & R. Garnett (Eds.), *Advances in neural information processing systems (nips)* (pp. 1632–1640). Curran Associates, Inc.
- Giusti, A., Guzzi, J., Ciresan, D., He, F.-L., Rodriguez, J. P., Fontana, F., . . . Gambardella, L. (2016). A machine learning approach to visual perception of forest trails for mobile robots. *IEEE Robotics and Automation Letters*.
- Goodfellow, I., Shlens, J., & Szegedy, C. (2015). Explaining and harnessing adversarial examples. In *International conference on learning representations (iclr)*. Retrieved from <http://arxiv.org/abs/1412.6572>
- Gopalakrishnan, S., Marzi, Z., Madhow, U., & Pedarsani, R. (2018). *Combating adversarial attacks using sparse representations*.
- Gopi, S., Netrapalli, P., Jain, P., & Nori, A. (2013). One-bit compressed sensing: Provable support and vector recovery. In *Proceedings of the 30th international conference on international conference on machine learning - volume 28* (pp. III-154–III-162). JMLR.org.
- Guo, Y., Zhang, C., Zhang, C., & Chen, Y. (2018). Sparse dnns with improved adversarial robustness. In *Advances in neural information processing systems* (pp. 240–249).
- He, K., Zhang, X., Ren, S., & Sun, J. (2015). Delving deep into rectifiers: Surpassing human-level performance on imagenet classification. In *IEEE international conference on computer vision, ICCV 2015* (pp. 1026–1034).
- Kolchinsky, A., & Tracey, B. D. (2017). Estimating mixture entropy with pairwise distances. *CoRR*, abs/1706.02419. Retrieved from <http://arxiv.org/abs/1706.02419>
- Kolchinsky, A., Tracey, B. D., & Wolpert, D. H. (2017). Nonlinear information bottleneck. *CoRR*, abs/1705.02436. Retrieved from <http://arxiv.org/abs/1705.02436>
- Kurakin, A., Goodfellow, I. J., & Bengio, S. (2017). Adversarial machine learning at scale. In *International conference on learning representations (iclr)*. Retrieved from <https://arxiv.org/abs/1611.01236>
- LeCun, Y., & Cortes, C. (2010). MNIST handwritten digit database. <http://yann.lecun.com/exdb/mnist/>.
- Litjens, G. J. S., Kooi, T., Bejnordi, B. E., Setio, A. A. A., Ciompi, F., Ghafoorian, M., . . . Sánchez, C. I. (2017). A survey on deep learning in medical image analysis. *CoRR*, abs/1702.05747. Retrieved from <http://arxiv.org/abs/1702.05747>

- Madry, A., Makelov, A., Schmidt, L., Tsipras, D., & Vladu, A. (2018). Towards deep learning models resistant to adversarial attacks. In *International conference on learning representations (iclr)*.
- Marzi, Z., Gopalakrishnan, S., Madhow, U., & Pedarsani, R. (2018). *Sparsity-based defense against adversarial attacks on linear classifiers*. Retrieved from <https://arxiv.org/abs/1801.04695>
- Moosavi-Dezfooli, S.-M., Fawzi, A., Fawzi, O., & Frossard, P. (2017). Universal adversarial perturbations. *2017 IEEE Conference on Computer Vision and Pattern Recognition (CVPR)*, 86-94.
- Moosavi-Dezfooli, S.-M., Fawzi, A., Fawzi, O., Frossard, P., & Soatto, S. (2018). Robustness of classifiers to universal perturbations: A geometric perspective. In *International conference on learning representations (iclr)*.
- Rozsa, A., Günther, M., & Boulton, T. E. (2016). Are accuracy and robustness correlated. *2016 15th IEEE International Conference on Machine Learning and Applications (ICMLA)*, 227-232.
- Rozsa, A., Günther, M., & Boulton, T. E. (2016). Towards robust deep neural networks with BANG. *CoRR*, *abs/1612.00138*.
- Sabour, S., Cao, Y., Faghri, F., & Fleet, D. J. (2016). Adversarial manipulation of deep representations.
- Sanyal, A., Kanade, V., & Torr, P. H. S. (2018). Low rank structure of learned representations. *CoRR*, *abs/1804.07090*. Retrieved from <http://arxiv.org/abs/1804.07090>
- Shwartz-Ziv, R., & Tishby, N. (2017). Opening the black box of deep neural networks via information. *CoRR*, *abs/1703.00810*. Retrieved from <http://arxiv.org/abs/1703.00810>
- Silver, D., Schrittwieser, J., Simonyan, K., Antonoglou, I., Huang, A., Guez, A., ... Hassabis, D. (2017, October). Mastering the game of go without human knowledge. *Nature*, *550*, 354-.
- Szegedy, C., Zaremba, W., Sutskever, I., Bruna, J., Erhan, D., Goodfellow, I., & Fergus, R. (2014). Intriguing properties of neural networks. In *International conference on learning representations (iclr)*.
- Sünderhauf, N., Brock, O., Scheirer, W., Hadsell, R., Fox, D., Leitner, J., ... Corke, P. (2018). The limits and potentials of deep learning for robotics. *The International Journal of Robotics Research*, *37*(4-5), 405-420. Retrieved from <https://doi.org/10.1177/0278364918770733> doi: 10.1177/0278364918770733
- Tanay, T., & Griffin, L. D. (2016). A boundary tilting perspective on the phenomenon of adversarial examples. *CoRR*, *abs/1608.07690*.
- Tishby, N., & Zaslavsky, N. (2015). Deep learning and the information bottleneck principle. *2015 IEEE Information Theory Workshop (ITW)*, 1-5.
- Tramèr, F., Papernot, N., Goodfellow, I. J., Boneh, D., & McDaniel, P. D. (2017). The space of transferable adversarial examples. *CoRR*, *abs/1704.03453*.
- Xiao, H., Rasul, K., & Vollgraf, R. (2017). Fashion-mnist: a novel image dataset for benchmarking machine learning algorithms. *CoRR*, *abs/1708.07747*. Retrieved from <http://arxiv.org/abs/1708.07747>
- Xiong, W., Droppo, J., Huang, X., Seide, F., Seltzer, M. L., Stolcke, A., ... Zweig, G. (2017, Dec). Toward human parity in conversational speech recognition. *IEEE/ACM Transactions on Audio, Speech, and Language Processing*, *25*(12), 2410-2423. doi: 10.1109/TASLP.2017.2756440

A Additional Experiments

Tables 1 and 2 are self-explanatory.

| Method | Test accuracy (on clean data) |
|--|----------------------------------|
| Natural train. | 0.9508 |
| FGSM adv. train. | 0.9697 |
| PGD adv. train. | 0.9689 |
| $\lambda_{1,1} = 0.01$ | 0.9527 |
| $\lambda_{*,1} = 0.01$ | 0.9681 |
| $\lambda_{1,1} = 0.01, \lambda_{*,1} = 0.01$ | 0.9446 |
| $\lambda_{1,1} = 0.01, \lambda_{*,1} = 0.03$ | 0.9327 |

Table 1: Test accuracies FCNN. Dataset: MNIST.

| Method | Test accuracy (on clean data) |
|--|----------------------------------|
| Natural train. | 0.9041 |
| FGSM adv. train. | 0.8639 |
| PGD adv. train. | 0.864 |
| $\lambda_{1,1} = 0.01, \lambda_{1,2} = 0.01, \lambda_{*,2} = 0$ | 0.8917 |
| $\lambda_{1,1} = 0.01, \lambda_{1,2} = 0.01, \lambda_{*,2} = 0.05$ | 0.8623 |
| $\lambda_{1,1} = 0.01, \lambda_{1,2} = 0.01, \lambda_{*,2} = 0.1$ | 0.8614 |
| $\lambda_{1,1} = 0.01, \lambda_{1,2} = 0.01, \lambda_{*,2} = 0.5$ | 0.8399 |

Table 2: Test accuracies CNN. Dataset: F-MNIST.

B Reshaping of Convolutional Filters

Assume a hidden representation composed of non-overlapping 3-dimensional patches X_1, \dots, X_m . A convolution operation is performed using 3-dimensional weight tensors W_1, \dots, W_n of the same size as the patches, which results in the following (vectorized) output of the convolution

$$\begin{aligned}
 & \begin{pmatrix} \text{vec}(W_1)^T \text{vec}(X_1) \\ \text{vec}(W_1)^T \text{vec}(X_2) \\ \vdots \\ \text{vec}(W_n)^T \text{vec}(X_m) \end{pmatrix} \\
 &= \underbrace{\begin{pmatrix} \text{vec}(W_1)^T \\ \text{vec}(W_2)^T \\ \vdots \\ \text{vec}(W_n)^T \end{pmatrix}}_{=: \widetilde{W}} \otimes I_m \begin{pmatrix} \text{vec}(X_1) \\ \text{vec}(X_2) \\ \vdots \\ \text{vec}(X_m) \end{pmatrix} \in \mathbb{R}^{mn}.
 \end{aligned}$$

Therefore, this convolution operation can be written as a standard fully connected layer with weight matrix $W = \widetilde{W} \otimes I_m$. Note that W and \widetilde{W} have the same effective rank, and \widetilde{W} is a reshaped version of the 4-dimensional weight tensor composed of W_1, \dots, W_n . Therefore, the matrix \widetilde{W} is used in (6) and (7) to regularize convolutional layers.